Catalysis Communications 57 (2014) 40–44

Contents lists available at ScienceDirect

Catalysis Communications

journal homepage: www.elsevier.com/locate/catcom

Short Communication

Selective liquid-phase hydrogenation of maleic anhydride to succinic anhydride on biosynthesized Ru-based catalysts

Yao Ma, Yangqiang Huang, Youwei Cheng *, Lijun Wang, Xi Li

Department of Chemical and Biological Engineering, Zhejiang University, Hangzhou 310027, PR China

ARTICLE INFO

Article history:
Received 15 June 2014
Received in revised form 29 July 2014
Accepted 1 August 2014
Available online 7 August 2014

Keywords:
Maleic anhydride
Hydrogenation
Succinic anhydride
Ruthenium nanoparticles

ABSTRACT

Ru-based catalysts, supported on activated carbon and carbon nanotubes, were synthesized by a simple and eco-friendly bioreduction method and tested in the liquid-phase hydrogenation of maleic anhydride. Over 2.0% Ru/AC, succinic anhydride was produced with a maximum yield of 99.2% without further hydrogenation to γ-butyrolactone. Well-defined spherical shapes with uniform small size of Ru nanoparticles and the residual plant biomass were responsible for the excellent catalytic activities and stabilities.

1. Introduction

Hydrogenation of maleic anhydride (MA) is an important industrial chemical process since MA can be produced with a large scale, high efficiency and low cost by the construction of large fluid bed plants, according to the Alusuisse–Lummus and BP/UCB technologies [1–3]. The global reaction network for MA hydrogenation is described in Fig. 1 [4], in which, both hydrogenation and hydrogenolysis reactions are involved. The products, such as succinic anhydride (SA), γ-butyrolactone (GBL), 1,4-butanediol (BDO) and tetrahydrofuran (THF), are valuable in ushering in a wide market in pharmaceutical and polymer industries [5]. Among a series of MA derivatives, SA is normally used in the manufacturing of polymers, agrochemicals, and pharmaceuticals [6,7]. These compounds are produced by mainly four processes: (a) Reppe process based on acetylene-formaldehyde condensation; (b) Acro process based on isomerization of propylene oxide to allyl alcohol and subsequent hydroformylation; (c) Mitsubishi Kasei process (MKC) based on the hydrogenation of maleic anhydride on Ru complexes; (d) Davy McKee process based on hydrogenation of dimethyl or diethyl maleates over Cu based catalysts [6,8]. However, these processes present some disadvantages. The Reppe process uses acetylene and formaldehyde as starting materials, and it uses severe reaction conditions (140–280 bar, 250–350 °C) [9]. The Davy McKee process needs two different reactors, catalysts and reaction conditions [10]. Generally, the hydrogenation reaction was carried out by using several types of noble metal-based catalysts, such as Pd, Pt, Ru, and Au or by copper-based catalysts, accompanied with chromium in both liquid and gas phase [10–14]. Cr-containing catalysts are getting increasingly difficult to use owing to their toxicity. Ru nanoparticles have attracted a great deal of attention because even under mild conditions they are one of the most active catalysts among the noble metals. In recent years, Ru nanoparticles including both unsupported and supported on carbon nanotubes, aluminum oxide, or other matrixes, have been synthesized and investigated. Antonetti et al. prepared supported ruthenium nanoparticles using a low boiling alcohol as solvent/reducing agent under microwave irradiation as heating source and successfully applied them to the selective hydrogenation of p-chloronitrobenzene to p-chloroaniline under mild reaction conditions [15]. Jeong used Ru-Ni/SiO_2 as catalysts in tetrahydrofuran at 240 °C and 7 MPa of H_2 for selective hydrogenation of MA to SA; SA was produced as the main product (73.2 wt.%) in accompany with the formation of GBL (8.7 wt.%) and other products, such as BDO [16].

Synthesis of nanoparticles (NPs) with biological entities such as plants and microorganisms has garnered much attention due to their unusual optical, chemical, photoelectrochemical, and electronic properties [17,18]. Moreover, the increasing environmental concerns necessitate the development of eco-friendly technologies in material syntheses. Compared with microorganisms, the biosynthesis of NPs utilizing the plants turns out to be simpler and much more available. After reviewing the progress of green synthesis of metal nanoparticles using different plants, Iravani found that the metal nanoparticles produced by plants are more stable in comparison with the traditional chemical and physical synthetic methods. Further from that, he drew the conclusion on the merits of using plant extract in scale-up and industrial production of well-dispersed metal nanoparticles [19]. Huang et al. demonstrated the biosynthesis of gold nanoparticles supported over TS-1 and successfully applied them to the epoxidation of styrene [20].

---

* Corresponding author. Tel.: +86 571 87952210; fax: +86 571 87951227.
E-mail address: ywcheng@zju.edu.cn (Y. Cheng).

http://dx.doi.org/10.1016/j.catcom.2014.08.001
1566-7367/

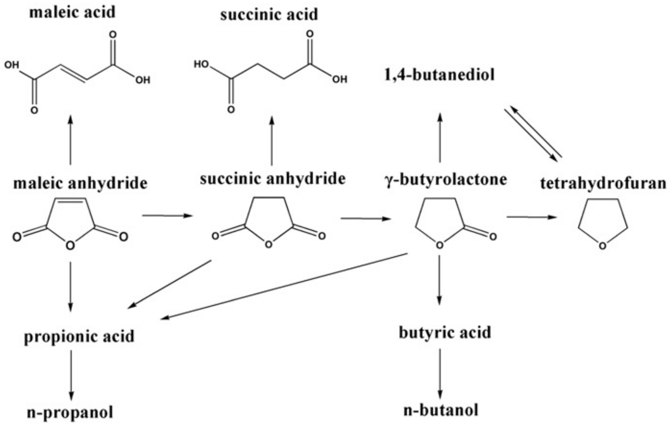

Fig. 1. Reaction network of hydrogenation of maleic anhydride.

This could be listed as one of the few successes in applying the biosynthesized nanoparticles to catalytic system.

Among the different types of supports used in heterogeneous catalysis, carbon materials enjoy a rising popularity due to their unique characteristics. Recently, new carbon form like the carbon nanotubes (CNTs) has generated an intense effervescence in the scientific community [21–26]. Hence, the aim of this work is to apply the simple bioreduction method to synthesizing highly efficient, stable and more economical carbon-supported Ru-based catalysts, to further boost the hydrogenation of MA to SA. As a preliminary result, these bioreduction catalysts were proved to be a candidate for the highly selective hydrogenation of MA to SA.

2. Experimental details

2.1. Catalyst preparation

Ru-based catalysts were prepared by the adsorption–reduction method using *Cacumen Platycladi* (*CP*) leaf extract. An aqueous $RuCl_3$ solution (50 mL, 2.2 mM) containing appropriate amount of the as-received AC or CNTs was treated in a water bath (60 °C) for 1 h, and then, 30 mL *CP* extract was added to reduce $RuCl_3$. After another 5 h, the suspension was filtered, and the residual filter cake was washed thoroughly with distilled water. All the catalysts were dried overnight at 100 °C and calcined in nitrogen at 500 °C for 3 h.

2.2. Catalysts characterization

N_2 adsorption–desorption isotherms were obtained on a Micromeritics ASAP 2020 instrument at liquid nitrogen temperature (− 196 °C). Transmission electron microscopy (TEM) was carried out on a Tecnai G2 F20 S-TWIN (FEI) at an accelerating voltage of 200 kV. X-ray diffraction (XRD) was performed on a Shimadzu powder X-ray diffractometer with Cu Kα radiation. Thermogravimetric (TG) analysis was carried out on a METTLER TGA/SDTA 851^e thermobalance under flowing N_2 atmosphere.

2.3. Catalyst test

The catalytic performance of the catalyst samples for liquid hydrogenation of MA to SA was carried out in a 100 mL capacity stainless steel batch reactor. The reactor was filled with the appointed maleic anhydride dissolved in 5 mL tetrahydrofuran (20 wt.%) and the catalyst loading used in the catalytic tests was 0.05 g. The reactor was purged with nitrogen to remove air. After the autoclave was heated up to the reaction temperature of 150 °C, the desired pressure of H_2 was introduced. Upon completion of the reaction, the reactor was rapidly cooled after treated in water baths and depressurized with a connected pressure regulator. Liquid samples were centrifuged to separate the catalysts from the mixture and then analyzed by gas chromatography on a gas chromatograph (Kexiao, GC-1690). ICP-AAS experiment was introduced to investigate the amount of ruthenium leaching after the reaction. Turnover frequency (TOF) value was calculated as moles of maleic anhydride transformed per mole of Ru in catalysts per hour.

3. Results and discussion

3.1. Catalysts characterization

An overview of the biosynthesized catalyst samples and their different characteristics was given in Table 1. The nitrogen adsorption–desorption results (Fig. S1 and S2) indicated that the activated carbon and the carbon nanotubes were distinct from one another in the average pore size and the surface area. After introducing the ruthenium particles, the BET surface and the pore volume in the two different supports decreased, indicating Ru nanoparticles partially occupied the mesopores of the supports. Analysis of the average pore size indicated that the Ru nanoparticles played a pivotal role in slightly extension of the catalyst pores. The diverse textural properties of the supports might have an influence on the catalytic properties.

Fig. 2 showed the TEM and HR-TEM images of the bioreduction catalysts. Well-defined spherical shapes with uniform size of Ru nanoparticles were produced by reducing $RuCl_3$ with the *C. Platycladi* (*CP*) leaf extract. Strikingly, from the histogram of their size distribution, a slightly smaller Ru size was obtained on the activated carbon compared with the carbon nanotubes. From the EDX analysis (Fig. 3), the ruthenium peak clearly confirms the existence of ruthenium in the catalysts. On the basis of the EDX results, ruthenium nanoparticles have been successfully prepared by using CP extract.

The XRD pattern of the two catalysts exhibited the standard peaks of carbon with the literature data (Fig. 4) [27,28]. No peaks, however, were detected for Ru species, indicating low percentage of ruthenium or well dispersion of the Ru nanoparticles on the supports.

Thermal analyses of the sample were introduced to ascertain the content of the residue plant biomass on the bioreduction catalysts (Fig. 5). The TG and DTG analyses indicated that plant biomass weighted as 13.5 (26.0) wt.% on uncalcined AC(CNTs) support, against only 6.1 (15.0) wt.% on calcined AC(CNTs) support. An appropriate content of the residue plant biomass might play an important role in preventing the sintering of the ruthenium particles [29]. FTIR analysis of the CP extract before bioreduction and the residue plant biomass showed that the functional groups of $C{=}C-H$ or $-C-O-H$ in the plant extract were responsible for the reduction of Ru(III). Therefore, we speculated that the polyols, such as reducing sugars and flavonoids, played a role in the bioreduction [30]. In addition, these functional groups could be adsorbed on the surface of the Ru nanoparticles to avoid agglomeration [31]. The analysis of the TG diagram suggested that the two supports possessed different adsorption properties, which might call for different calcination treatments in nitrogen.

Table 1
Textural properties of the supports and synthesized catalysts.

Sample	Ru loading (wt.%)[a]	Surface area ($m^2 \cdot g^{-1}$)	Pore volume ($cm^3 \cdot g^{-1}$)	Average pore size (nm)
Activated carbon (AC)	–	907	0.64	3.7
1.0% Ru/AC	1.0	845	0.61	3.8
2.0% Ru/AC	2.0	779	0.58	4.0
Carbon nanotube (CNT)	–	221	1.44	15.8
1.0% Ru/CNT	1.0	216	1.05	19.2
2.0% Ru/CNT	2.0	194	0.93	19.4

[a] Determined by ICP-AAS.